

# First-Principles Calculations of Luminescence Spectrum Line Shapes for Defects in Semiconductors: The Example of GaN and ZnO

Audrius Alkauskas, John L. Lyons, Daniel Steiauf, and Chris G. Van de Walle

Materials Department, University of California, Santa Barbara, California 93106-5050, USA

(Received 11 September 2012; published 28 December 2012)

We present a theoretical study of the broadening of defect luminescence bands due to vibronic coupling. Numerical proof is provided for the commonly used assumption that a multidimensional vibrational problem can be mapped onto an effective one-dimensional configuration coordinate diagram. Our approach is implemented based on density functional theory with a hybrid functional, resulting in luminescence line shapes for important defects in GaN and ZnO that show unprecedented agreement with experiment. We find clear trends concerning effective parameters that characterize luminescence bands of donor- and acceptor-type defects, thus facilitating their identification.

DOI: 10.1103/PhysRevLett.109.267401

PACS numbers: 78.55.Cr, 61.72.Bb, 63.20.kp, 71.55.-i

Defects play a key role in the properties of solids. From the early days of color centers, the study of luminescence and absorption has been crucial to defect characterization [1]. Theoretical efforts to calculate the broadening of optical transitions at defects due to the interactions with lattice vibrations were pioneered by Huang and Rhys [2] and Pekar [3]. While those theories and their generalizations [1,4] have been very successful in describing the shape of experimental optical bands [1,5], this inevitably required the use of empirical fitting parameters. Theory has thus been limited in its ability to aid the microscopic identification of defects or produce accurate predictions.

In this Letter, we report that unprecedented precision can now be achieved by rigorously mapping the multidimensional vibrational problem onto an effective one-dimensional configuration coordinate diagram, combined with advanced electronic structure techniques [6,7]. We demonstrate the power of the approach with the example of a number of defects in GaN [5] and ZnO [8], two technologically crucial wide-band-gap semiconductors. Excellent agreement with experiment is achieved for well-characterized defects, and new insights into vibronic coupling emerge.

Our electronic structure calculations are based on density functional theory using the hybrid functional of Ref. [7] in the VASP code [9]. The fraction  $\alpha$  of the screened Fock exchange admixed to the semilocal exchange was set to 0.31 for GaN and 0.36 for ZnO to obtain band gaps very close to experimental ones (3.5 and 3.3 eV). By describing bulk electronic structure better and reducing self-interaction errors, hybrid functionals substantially improve the accuracy of defect calculations [10–12]. Defects were treated via the supercell approach [6], the interaction with nuclei was described within the projector-augmented wave formalism [9], and electron wave functions were expanded in plane waves with a cutoff of 400 eV. Normal modes and frequencies have been calculated by using finite differences.

We illustrate the methodology with the example of the  $\text{Mg}_{\text{Ga}}$  acceptor in GaN, a crucial defect since it is the only acceptor impurity capable of making the material *p* type. While *electrically* acting as a shallow impurity with modest ionization energy, *optically*  $\text{Mg}_{\text{Ga}}$  behaves as a deep center [13]: Recombination of an electron at the conduction-band minimum with a hole localized on the neutral  $\text{Mg}_{\text{Ga}}^0$  acceptor gives rise to a broad blue luminescence band [13]. The calculated zero-phonon line (ZPL) energy (see Fig. 1) is 3.24 eV. We assume here that optical transitions start with a delocalized charge carrier; excitonic effects are small [14].

The general theory of luminescence was described in Refs. [1,2,4]. When optical transitions are dipole allowed, as is the case for the defects studied in this work, at finite *T*

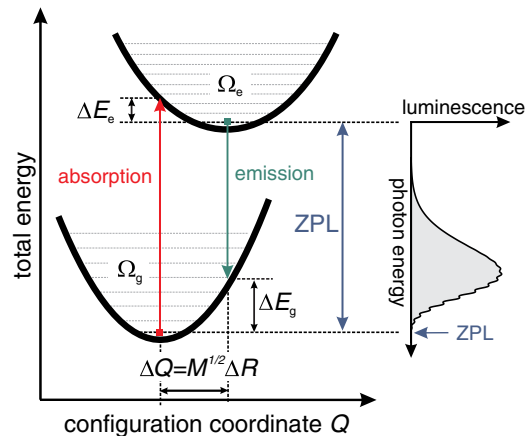


FIG. 1 (color online). 1D configuration coordinate diagram describing optical absorption and emission at a point defect. The minima of the ground-state and excited-state potential energy surfaces are displaced.  $\Delta E_{\{e,g\}}$  are the relaxation energies and  $\Omega_{\{e,g\}}$  the effective phonon frequencies. ZPL indicates the zero-phonon line, i.e., the transition between the zero-point vibrational states in excited- and ground-state configurations.

the normalized luminescence intensity (line shape) in the leading order can be written as  $G(\hbar\omega) = C\omega^3 A(\hbar\omega)$ , where  $A(\hbar\omega)$  is the normalized spectral function

$$A(\hbar\omega) = \sum_{m,n} w_m(T) |\langle \chi_{em} | \chi_{gn} \rangle|^2 \times \delta(E_{ZPL} + \hbar\omega_{em} - \hbar\omega_{gn} - \hbar\omega), \quad (1)$$

and  $C^{-1} = \int A(\hbar\omega) \omega^3 d(\hbar\omega)$ . The sum runs over all vibrational levels with energies  $\hbar\omega_{em}$  and  $\hbar\omega_{gn}$  of the excited and the ground state [ $w_m(T)$  being thermal occupation of the former],  $\chi$  are ionic wave functions, and  $E_{ZPL}$  is the energy of the ZPL. Such a formulation constitutes the Franck-Condon approximation in which it is assumed that the electronic transition dipole moment is independent of ionic coordinates [1].

Evaluation of  $A(\hbar\omega)$  is complicated by the fact that, first, the sum includes all relevant vibrational degrees of freedom and, second, normal modes  $\mathbf{Q}_e$  and  $\mathbf{Q}_g$  in the excited and the ground state are usually not identical. The two are related via the Duschinsky transformation  $\mathbf{Q}_e = \mathbf{J}\mathbf{Q}_g + \Delta\mathbf{Q}$  [15], and  $\langle \chi_{em} | \chi_{gn} \rangle$  are thus highly multidimensional integrals. For small molecular systems, recursive techniques to calculate such integrals have been developed [16] and implemented [17]. The large number of vibrational modes that occur for defects in solids render such a direct approach computationally prohibitive.

Broad optical bands have most often been described via 1D configuration-coordinate diagrams [1,4] [Fig. 1], based on the assumption that the large number of vibrational modes (with different frequencies) contributing to the line shape can be replaced by a single effective mode (sometimes a small number of modes). The parameters entering the 1D model are the modal mass  $M$  of the effective vibration, the displacement of the potential energy minima  $\Delta R$ , and the effective frequencies  $\Omega_g$  and  $\Omega_e$  [Fig. 1]. Based on these, the widely used ‘‘Huang-Rhys (HR) factors’’ [2] are defined as the average number of phonons created during a vertical transition:  $S_g = \Delta E_g / \hbar\Omega_g$  and  $S_e = \Delta E_e / \hbar\Omega_e$ . There are many examples where a 1D model with empirical fitting parameters provides a good approximation to experimental luminescence line shapes [1,5]; still, because it is strictly valid only when all the modes have the same frequency [2], its general applicability has often been questioned. More importantly, the use of fitting parameters precludes linking to potentially valuable microscopic information about the defect and limits the predictive power.

Here we address this problem by using the following strategy. Vibrations that couple strongly to the distortion of the geometry are expected to be dominant in  $A(\hbar\omega)$ . Such modes have finite weight on the atoms that experience the largest relaxations, i.e., the atoms close to the defect. When only a small number of atoms are included in calculating vibrations,  $\langle \chi_{em} | \chi_{gn} \rangle$  can be evaluated exactly, taking

mode mixing into account [16,17]. This exact evaluation can then serve as a test of the accuracy of any approximations. Once an approximate treatment has been validated in this fashion, it can be applied to much larger systems of atoms provided it is sufficiently less numerically demanding than the exact evaluation.

In the case of  $\text{Mg}_{\text{Ga}}^0$ , a hole is localized on an N neighbor of the Mg atom, and the five atoms surrounding this hole account for more than 90% of the whole relaxation. The calculated luminescence line shape, taking mixing between the resulting 15 vibrations into account, is shown in Fig. 2. Multidimensional overlap integrals were calculated by using the MOLFC code [17]. We have applied a Gaussian smearing with a small  $\sigma = 0.01$  eV to simulate additional broadening mechanisms, resulting in a smooth line shape.

Recursive algorithms [16] lead to exploding computational requirements when applied to larger atom clusters. A simplification that is often used for molecules [17] and almost always implied in solids [4] is the parallel-mode approximation, in which the eigenmodes of either the ground state or the excited state are chosen as common vibrational states, leading to  $\mathbf{J} = \mathbf{1}$ .  $\langle \chi_{em} | \chi_{gn} \rangle$  then factorizes into 1D integrals, each corresponding to one vibrational mode, greatly reducing computational complexity. As seen in Fig. 2, the resulting line shape is indeed close to the exact result. Therefore, while mode mixing is present, it is not substantial.

Now that we have validated the parallel-mode approximation, we can include more atoms, since overlap integrals become easy to calculate. However, the number of terms that have to be included grows very rapidly with system size. This reflects the fact that important modes often do not occur in the gap of the bulk phonon spectrum but are resonances and therefore not well localized in real space. Consequently, further approximations are required. This we achieve by devising a suitable 1D configuration-coordinate diagram based on computed parameters as outlined below.

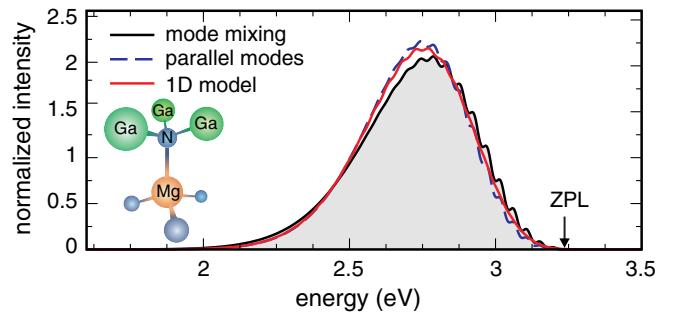


FIG. 2 (color online). Normalized luminescence spectrum of the  $\text{Mg}_{\text{Ga}}(0/-)$  transition, calculated by taking into account vibrational modes of only those atoms that relax most (labeled in the inset). Black solid line (and shaded area): Calculation including mode mixing; blue dashed line: parallel-mode approximation; red solid line: effective 1D vibrational problem.

The weight by which each normal mode  $k$  contributes to the distortion of the defect geometry during optical transition can be written as  $p_k = (\Delta Q_k / \Delta Q)^2$ , where

$$\Delta Q_k = \sum_{\alpha i} m_{\alpha}^{1/2} \Delta R_{\alpha i} q_{k;\alpha i}; \quad (\Delta Q)^2 = \sum_k \Delta Q_k^2. \quad (2)$$

Here  $\alpha$  labels atoms,  $i = \{x, y, z\}$ ,  $\Delta R_{\alpha i} = R_{e;\alpha i} - R_{g;\alpha i}$  is the distortion vector,  $R_{\{e,g\};\alpha i}$  are atomic coordinates, and  $q_{k;\alpha i}$  is the unit vector in the direction of the normal mode  $k$  ( $\sum_{\alpha i} q_{k;\alpha i} q_{l;\alpha i} = \delta_{k,l}$ ). We find that it is useful to define an effective frequency

$$\Omega_{\{e,g\}}^2 = \langle \omega_{\{e,g\}}^2 \rangle = \sum_k p_{\{e,g\};k} \omega_{\{e,g\};k}^2 \quad (3)$$

where  $\omega_{\{e,g\};k}$  is the frequency of the mode  $q_{\{e,g\};k}$ .

Parameters  $E_{ZPL}$ ,  $\Delta Q$ ,  $\Omega_g$ , and  $\Omega_e$  define a 1D configuration-coordinate diagram (cf. Fig. 1) for a quantum oscillator with unit mass and can be used to calculate the luminescence line shape. Gaussian smearing is still applied, but it should now reflect the replacement of many vibrations at various frequencies with one effective frequency. Inspection of the mean-square deviation for the distribution of phonon frequencies that contribute to the distortion leads to  $\sigma = 0.025$  eV ( $\sim 0.6\hbar\Omega_g$ ). The result for  $\text{Mg}_{\text{Ga}}$  in Fig. 2 shows that our rigorously defined 1D model is an excellent approximation to the multidimensional calculations.

Now that the validity of the 1D model has been established, it can be extended to larger numbers of atoms, and we no longer need to explicitly calculate normal modes and frequencies to determine the effective parameters  $\Delta Q$  [Eq. (2)] and  $\Omega_{\{e,g\}}$  [Eq. (3)]. Indeed, by inserting the expression for  $\Delta Q_k$  into the one for  $\Delta Q$  in Eq. (2), one can show that, when all the atoms in the supercell are included in the vibrational problem,  $(\Delta Q)^2 = \sum_{\alpha,i} m_{\alpha} \Delta R_{\alpha i}^2$ . The modal mass is defined via  $\Delta Q = M^{1/2} \Delta R$ , where  $(\Delta R)^2 = \sum_{\alpha,i} \Delta R_{\alpha i}^2$ . Effective frequencies

$\Omega$  can be obtained by mapping the potential energy surface around the respective equilibrium geometries along the path that linearly interpolates between the two geometries [18]. A third-order polynomial fit was found to suffice in all cases. The frequency  $\Omega$  in the quadratic term defined in this way is equivalent to the one calculated from Eq. (3). In the case of low-temperature spectra, third-order anharmonic corrections that affect vibrational wave functions and thus overlap integrals were included in the calculations of the spectral function perturbatively. For all subsequent calculations, we have used 96-atom wurtzite supercells, and relaxations of all the atoms were included in determining effective parameters. The resulting parameters are summarized in Table I.

The luminescence line shape  $G(\hbar\omega)$  for  $\text{Mg}_{\text{Ga}}$  at  $T = 0$  K is shown in Fig. 3(a), together with experimental low-temperature data from Refs. [19,20]. To facilitate comparison with experiment, the calculated line shapes were shifted to bring the maximum of the luminescence in agreement with that of the experimentally measured curves. The magnitude of the shift provides an estimate for the error in the  $E_{ZPL}$  (thermodynamic transition level) and is less than 0.12 eV for all defects. This error bar reflects both the remaining inaccuracy of even the most advanced first-principles methods and any electrostatic corrections (such as excitonic effects or donor-acceptor interactions) not included in the present model. The width of the theoretical band (0.44 eV) is only slightly larger than the experimental value of 0.36–0.37 eV. We derive the effective vibrational frequency in the ground state  $\hbar\Omega_g = 47$  meV, and the HR factor  $S_g = 12.2$ . Overall, the good agreement between the calculated and experimental line shapes for  $\text{Mg}_{\text{Ga}}$  attests to the power of the approach presented here, when used in combination with state-of-the-art density functional calculations.

The agreement with experiment is even better for our second example,  $\text{C}_{\text{N}}$ . This defect has been suggested as a source of yellow luminescence (YL) [5,22,23] based on the

TABLE I. Effective parameters for various defect-related luminescence transitions in GaN and ZnO.  $\Delta Q$  and  $\Delta R$ : Total mass-weighted and total distortions;  $M$ : modal mass;  $\hbar\Omega_{\{e,g\}}$ : effective frequencies in the ground and excited states (charge state in parentheses);  $E_{ZPL}$ : zero-phonon line energy; FWHM: full width at half maximum of the band;  $T$ : temperature for which the FWHM is given;  $S_{\{e,g\}}$ : Huang-Rhys factors. If experimental parameters are not explicitly given in the corresponding experimental papers, they are extracted by using the original data and are shown in italics.

Defect, charge states, and optical transition	Method	$\Delta Q$ (amu <sup>1/2</sup> Å)	$M$ (amu)	$\Delta R$ (Å)	$\hbar\Omega_g$ (meV)	$\hbar\Omega_e$ (meV)	$E_{ZPL}$ (eV)	FWHM at $T$ (eV, K)	$S_g$	$S_e$
$\text{Mg}_{\text{Ga}}$ (0/−) in GaN	Theory	1.59	45	0.24	47 (−)	34 (0)	3.24 [13]	0.44 at 0 K	12.2	...
$\text{Mg}_{\text{Ga}}^0 + e^- \rightarrow \text{Mg}_{\text{Ga}}^-$	Expt.						3.30 [19]	0.36 at 13 K [19]		
							3.36 [20]	0.37 at 8 K [20]		
$\text{C}_{\text{N}}$ (0/−) in GaN	Theory	1.55	51	0.22	42 (−)	36 (0)	2.60 [21]	0.35 at 77 K	11.2	10.3
$\text{C}_{\text{N}}^0 + e^- \rightarrow \text{C}_{\text{N}}^-$	Expt.				41 ± 5	40 ± 5 [22]	2.64 [22]	0.39 at 77 K [23]	12.8 ± 1.6	13.4 ± 1.7 [22]
$\text{V}_{\text{N}}$ (+3/+2) in GaN	Theory	3.72	68	0.45	23 (+2)	21 (+3)	3.02 [24]	0.33 at 0 K	36.0	34.8
$\text{V}_{\text{N}}^{+3} + e^- \rightarrow \text{V}_{\text{N}}^{+2}$	Expt.						3.07 [25]	0.36 at 5 K [25]		
$\text{N}_{\text{O}}$ (0/−) in ZnO	Theory	1.92	48	0.28	40 (−)	32 (0)	2.20 [12]	0.54 at 300 K	15.3	15.1
$\text{N}_{\text{O}}^0 + e^- \rightarrow \text{N}_{\text{O}}^-$	Expt.						2.30 [26]	0.55 at 300 K [26]		

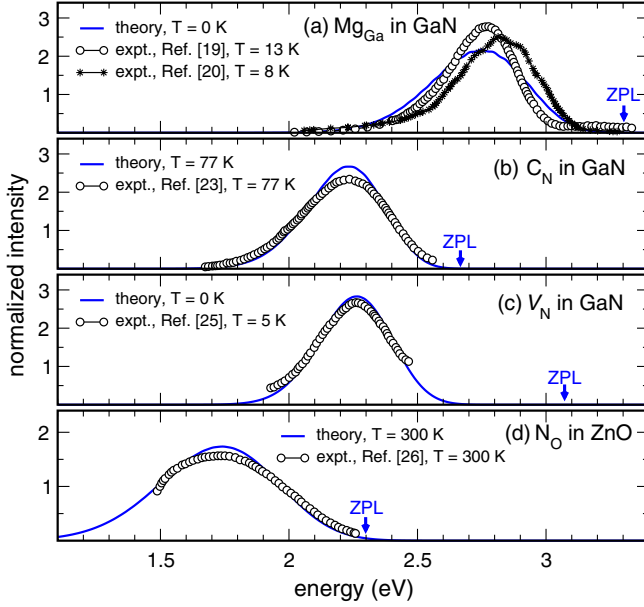


FIG. 3 (color online). Calculated (solid lines) and measured (symbols) luminescence line shapes for (a)  $\text{Mg}_{\text{Ga}}$  in GaN, (b)  $\text{C}_{\text{N}}$  in GaN, (c)  $\text{V}_{\text{N}}$  in GaN, and (d)  $\text{N}_{\text{O}}$  in ZnO. The arrows indicate the ZPL, and the calculated spectra were shifted by  $\sim 0.1$  eV, as discussed in the text. In (a), the experimental spectrum of Ref. [19] has been used as a reference in this procedure.

transition  $\text{C}_{\text{N}}^0 + e^- \rightarrow \text{C}_{\text{N}}^-$  [21] (where  $e^-$  is an electron at the conduction-band minimum). This defect again exhibits hole localization in the neutral charge state, but now the hole is localized on the C atom [21]. The calculated luminescence line shape at  $T = 77$  K [Fig. 3(b)] agrees very well with the measurements of Ref. [23], in which YL was convincingly attributed to a C-related defect. Our calculated effective frequencies ( $\hbar\Omega_{\{e,g\}} = 36, 42$  meV) and HR factors ( $S_{\{e,g\}} = 10.3, 11.2$ ) are in excellent agreement with those measured in Ref. [22] (Table I).

Our next example is  $\text{V}_{\text{N}}$ . Nitrogen vacancies have low formation energies in  $p$ -type GaN, and they have been suggested [24] as a cause of the YL in  $p$ -GaN observed in Ref. [25]. The calculated luminescence line shape for the transition  $\text{V}_{\text{N}}^{+3} + e^- \rightarrow \text{V}_{\text{N}}^{+2}$  [Fig. 3(c)] shows impressive agreement with these low-temperature experiments.

To demonstrate that the approach is not limited to GaN, in Fig. 3(d) we compare the calculated and measured [26] luminescence line shapes at  $T = 300$  K for the deep  $\text{N}_{\text{O}}$  acceptor in ZnO, corresponding to the transition  $\text{N}_{\text{O}}^0 + e^- \rightarrow \text{N}_{\text{O}}^{-1}$  [12]. The agreement between theory and experiment is again extremely good.

Our ability to calculate accurate parameters allows us to examine some general trends. For the two substitutional acceptors in GaN analyzed above, total distortions  $\Delta R$  amount to  $0.22$ – $0.24$  Å, and HR factors to  $10$ – $12$ , irrespective of whether the hole is bound to C or N. Other acceptors with anion-bound holes ( $\text{V}_{\text{Ga}}$ ,  $\text{Be}_{\text{Ga}}$ , and  $\text{Zn}_{\text{Ga}}$ ) show very similar behavior. The donor  $\text{V}_{\text{N}}$ , on the other hand, is very

different. Its defect wave function is composed mainly of Ga  $4s$  states, and  $\Delta R$  associated with the  $(+3/+2)$  transition is  $0.45$  Å, almost twice as large as in the case of acceptors. The distortion mostly affects the four nearest Ga atoms, leading to a large modal mass and small effective frequencies (Table I). In conjunction with large relaxation energies ( $0.72$  and  $0.82$  eV), this results in very large HR factors ( $S_{\{e,g\}} = 34.8, 36.0$ ). This is in contrast with the acceptors, where anions are involved in the distortion, leading to smaller modal masses, higher effective vibrational frequencies, and hence more than twice smaller HR factors. Similar trends are observed for ZnO: We find  $\hbar\Omega_{\{e,g\}} = 28$ – $40$  meV and  $S_{\{e,g\}} < 30$  for acceptors with anion-localized holes ( $\text{N}_{\text{O}}$ ,  $\text{V}_{\text{Zn}}$ , and  $\text{Li}_{\text{Zn}}$ ), while  $\hbar\Omega_{\{e,g\}} = 16, 21$  meV and  $S_{\{e,g\}} \approx 50$  for donors with cation-derived states ( $\text{V}_{\text{O}}$ ). The general result for acceptors in ZnO is in accord with experimental data of Ref. [27].

While such *a posteriori* interpretations are simple and intuitive, they are reliable only if based on an accurate microscopic description of the defect. We note that model calculations have yielded results that were very different from our first-principles values (e.g.,  $S = 3.5$ – $6.5$  for defects related to YL in Ref. [28]), starkly illustrating the shortcomings of such approaches.

High values of HR factors mean that it is very difficult to determine the ZPL in experimental luminescence spectra. Indeed, the weight of the ZPL is exponentially suppressed for larger  $S$ :  $|\langle \chi_{e0} | \chi_{g0} \rangle|^2 \approx \exp\{-S_{\{e,g\}}\}$  (equality holds for  $\Omega_g = \Omega_e$  [2]). As seen in Fig. 3, this complication arises for all the defects studied here and is especially apparent for  $\text{V}_{\text{N}}$ . This highlights the practical use of calculations exemplified in the current work.

The examples have demonstrated that our methodology is capable of producing luminescence line shapes in very good agreement with experiment, as well as quantities that can be directly compared with experimental parameters. The achieved agreement is based on the accuracy of the underlying electronic structure method but also on the applicability of the 1D model to broad luminescence bands. While the explicit consideration of many vibrational modes is sometimes needed to understand the experimental spectra when  $S \approx 1$  (i.e., defects with moderate electron-phonon coupling) [1,4,29], we have demonstrated that a 1D model with suitably calculated parameters is valid for defects with large electron-phonon coupling ( $S \gg 1$ ), even if many phonon modes couple to the optical transition. Our calculations have provided theoretical evidence that the effective mode frequency is usually indeed much smaller than that of longitudinal-optical (LO) phonons ( $91$  meV in GaN and  $73$  meV in ZnO), contrary to what has been often assumed in phenomenological approaches [2,28]. Our conclusion is in full agreement with detailed experimental measurements for color centers in alkali halides [30], indicating the generality of the obtained result.

Our findings are important for future studies of semiconductors and insulators that exhibit broad defect luminescence bands. In particular, the developed methodology will assist the identification of the microscopic origin of numerous as yet unassigned bands in technologically important wide-band-gap materials. More generally, our work attests to the success of first-principles methods to describe electron-phonon interactions in solids [31] beyond the application to perfect crystals.

We thank F. Bechstedt, N. Grandjean, A. Janotti, M. A. Reshchikov, and Q. Yan for discussions as well as A. Borelli for a copy of the MOLFC code. A. A. acknowledges a grant from the Swiss NSF (PA00P2-134127). D. S. was supported as part of the Center for Energy Efficient Materials, an Energy Frontier Research Center funded by the U.S. DOE, BES under Grant No. DE-SC0001009. Additional support was provided by NSF (DMR-0906805) and computational resources by XSEDE (NSF OCI-1053575 and DMR07-0072N) and NERSC (DOE Office of Science DE-AC02-05CH11231).

- 
- [1] A. M. Stoneham, *Theory of Defects in Solids* (Oxford University, New York, 1975).
- [2] K. Huang and A. Rhys, *Proc. R. Soc. A* **204**, 406 (1950).
- [3] S. I. Pekar, *Zh. Eksp. Teor. Fiz.* **20**, 510 (1950).
- [4] M. Lax, *J. Chem. Phys.* **20**, 1752 (1952); J. J. Markham, *Rev. Mod. Phys.* **31**, 956 (1959); I. S. Osad'ko, *Usp. Fiz. Nauk.* **128**, 21 (1979).
- [5] M. A. Reshchikov and H. Morkoç, *J. Appl. Phys.* **97**, 061301 (2005).
- [6] C. G. Van de Walle and J. Neugebauer, *J. Appl. Phys.* **95**, 3851 (2004).
- [7] J. Heyd, G. E. Scuseria, and M. Ernzerhof, *J. Chem. Phys.* **118**, 8207 (2003).
- [8] Ü. Özgür, Ya. I. Alivov, C. Liu, A. Teke, M. A. Reshchikov, S. Doğan, V. Avrutin, S.-J. Cho, and H. Morkoc, *J. Appl. Phys.* **98**, 041301 (2005).
- [9] G. Kresse and J. Furthmüller, *Phys. Rev. B* **54**, 11 169 (1996); G. Kresse and D. Joubert, *Phys. Rev. B* **59**, 1758 (1999).
- [10] G. Pacchioni, F. Frigoli, D. Ricci, and J. A. Weil, *Phys. Rev. B* **63**, 054102 (2001).
- [11] A. Alkauskas, P. Broqvist, and A. Pasquarello, *Phys. Rev. Lett.* **101**, 046405 (2008); *Phys. Status Solidi B* **248**, 775 (2011).
- [12] J. L. Lyons, A. Janotti, and C. G. Van de Walle, *Appl. Phys. Lett.* **95**, 252105 (2009).
- [13] J. L. Lyons, A. Janotti, and C. G. Van de Walle, *Phys. Rev. Lett.* **108**, 156403 (2012).
- [14] The exciton binding energy in bulk GaN is 0.021–0.023 eV, as measured in W. Shan, B. D. Little, A. J. Fischer, J. J. Song, B. Goldenberg, W. G. Perry, M. D. Bremser, and R. F. Davis, *Phys. Rev. B* **54**, 16 369 (1996).
- [15] F. Duschinsky, *Acta Physiochim. USSR* **7**, 551 (1937).
- [16] E. V. Doktorov, I. A. Malkin, and V. I. Man'ko, *J. Mol. Spectrosc.* **64**, 302 (1977).
- [17] R. Borrelli and A. Peluso, *J. Chem. Phys.* **119**, 8437 (2003).
- [18] F. Schanovsky, W. Göss, and T. Grasser, *J. Vac. Sci. Technol. B* **29**, 01A201 (2011).
- [19] M. A. Reshchikov, G.-C. Yi, and B. W. Wessels, *Phys. Rev. B* **59**, 13176 (1999).
- [20] M. Leroux, N. Grandjean, B. Beaumont, G. Nataf, F. Semond, J. Massies, and P. Gibart, *J. Appl. Phys.* **86**, 3721 (1999).
- [21] J. L. Lyons, A. Janotti, and C. G. Van de Walle, *Appl. Phys. Lett.* **97**, 152108 (2010).
- [22] T. Ogino and M. Aoki, *Jpn. J. Appl. Phys.* **19**, 2395 (1980).
- [23] C. H. Seager, D. R. Tallant, J. Yu, and W. Götz, *J. Lumin.* **106**, 115 (2004).
- [24] Q. Yan, A. Janotti, M. Scheffler, and C. G. Van de Walle, *Appl. Phys. Lett.* **100**, 142110 (2012).
- [25] G. Salviati, N. Armani, C. Zanotti-Fregonara, E. Gombia, M. Albrecht, H. P. Strunk, M. Mayer, M. Kamp, and A. Gasparott, *MRS Internet J. Nitride Semicond. Res.* **5S1**, W11.50 (2000).
- [26] M. C. Tarun, M. Zafar Iqbal, and M. D. McCluskey, *AIP Adv.* **1**, 022105 (2011).
- [27] M. A. Reshchikov, K. Garbus, G. Lopez, M. Ruchala, N. Nemeth, and J. Nause, *Mater. Res. Soc. Symp. Proc.* **957**, 0957-K07-19 (2006).
- [28] B. K. Ridley, *J. Phys. Condens. Matter* **10**, L461 (1998).
- [29] M. K. Kretov, I. M. Iskandarova, B. V. Potapkin, A. V. Scherbinin, A. M. Srivastava, and N. F. Stepanov, *J. Lumin.* **132**, 2143 (2012).
- [30] G. E. Russel and C. C. Klick, *Phys. Rev.* **101**, 1473 (1956).
- [31] F. Giustino, M. L. Cohen, and S. G. Louie, *Phys. Rev. B* **76**, 165108 (2007).